



This discussion paper is/has been under review for the journal Atmospheric Measurement Techniques (AMT). Please refer to the corresponding final paper in AMT if available.

Field deployable diode-laser-based differential absorption lidar (DIAL) for profiling water vapor

S. M. Spuler¹, K. S. Repasky², B. Morley¹, D. Moen², M. Hayman¹, and A. R. Nehrir³

¹National Center for Atmospheric Research, Earth Observing Lab, Boulder, CO 80307, USA

²Montana State University, Electrical and Computer Engineering, Bozeman, MT 59717, USA

³NASA Langley Research Center, Hampton, VA 23681, USA

Received: 26 August 2014 – Accepted: 27 October 2014 – Published: 18 November 2014

Correspondence to: S. M. Spuler (spuler@ucar.edu)

Published by Copernicus Publications on behalf of the European Geosciences Union.

Field deployable diode-laser-based DIAL for profiling water vapor

S. M. Spuler et al.

Title Page

Abstract

Introduction

Conclusions

References

Tables

Figures



Back

Close

Full Screen / Esc

Printer-friendly Version

Interactive Discussion



**Field deployable
diode-laser-based
DIAL for profiling
water vapor**

S. M. Spuler et al.

Title Page

Abstract

Introduction

Conclusions

References

Tables

Figures



Back

Close

Full Screen / Esc

Printer-friendly Version

Interactive Discussion



fidelity for DIAL measurements. Machol et al. demonstrated nighttime water vapor profiles up to 2.5 km with 30 min integration periods. Building from this initial modeling and instrument development, researchers at Montana State University (MSU) developed a series of diode-laser-based WV-DIAL instruments. The first generation utilized an external cavity diode laser (ECDL) and a passively pulsed amplifier (Nehrir et al., 2009). A second generation instrument achieved a factor of 10–20 greater energy (1–2 μJ) with a pulsed dual stage TSOA in a master oscillator power amplifier (MOPA) configuration (Nehrir et al., 2011). This version provided the first demonstration of daytime water vapor measurements with a diode-laser-based DIAL. A third generation, utilizing a pair of ECDLs connected via a fiber coupled MEMS switch to an improved single stage TSOA achieved an even greater pulse energy of 7 μJ (Nehrir et al., 2012). In all of these versions, the receiver utilized a commercial telescope to direct the collected light to an avalanche photodiode (APD) operating in the Geiger mode. Two narrow-band filters, each with a 250 pm full width half maximum (FWHM) bandpass were used to filter solar background allowing clear-sky daytime measurements to approximately 3 km.

Since the summer of 2011, the researchers at Montana State University (MSU) and the National Center for Atmospheric Research (NCAR) have collaborated to advance and evaluate the capability of the diode-laser-based WV-DIAL technique. In 2012, the MSU third generation WV-DIAL was modified to allow for unattended operations in a laboratory environment; replacing the external cavity diode lasers with more temperature robust distributed Bragg reflector (DBR) lasers, and expanding the beam to be eye-safe at the exit port. The redesigned transmit path for this temporary prototype used a series of large turning mirrors to reflect the expanded eye-safe beam into the receiver field-of-view and was subject pointing instability with environmental temperature fluctuations. Nevertheless, the modified prototype was field tested over a wide range of atmospheric conditions to evaluate its performance. The evaluation indicated that the technology was well-suited for autonomous, long term measurements of water vapor; however, as noted in Repasky et al. (2013), improvements to the instrument

2 Description of the field prototype

The instrument, shown schematically in Fig. 1, utilizes a diode-laser-based MOPA configured transmitter capable of rapid wavelength switching (red shading), a shared telescope transmitter and receiver to achieve opto-mechanically stable eye-safe operation (purple shading), and a multi-stage filtered two channel receiver for the near and far range returns (blue shading). The system parameters are outlined in Table 1.

2.1 Laser transmitter

The laser transmitter utilizes two DBR laser diodes, one operating at the online wavelength (828.2 nm) and the other operating at the offline wavelength (828.3 nm) These lasers operate in the continuous wave (cw) mode, produce up to 80 mW of power, and have a measured linewidth less than 1 MHz. The output from each diode is collimated using an aspheric lens and passes through a Faraday isolator to prevent unwanted feedback from affecting the power output and spectral stability. This seed laser light is then fiber coupled to allow for splitting and switching prior to pulsed amplification in the TSOA.

The third generation WV-DIAL instrument used a fiber coupled MEMS switch to alternate between the online and offline wavelength which exhibited a 1 ms 10/90 switching time as discussed in Nehrir et al. (2012). The data acquisition system utilized a single channel of a four channel scaler photon counting card which had 2 buffers to allow for continuous read and write operations to occur. To avoid mixing the signals within the data acquisition system – one laser frequency was transmitted for 3 s, followed a 3 s dead time when the wavelength switch was changed, then the other laser frequency was transmitted for 3 s. This switching method worked well, but it created several performance limitations. First, the dead time resulted in a 60 % duty cycle (i.e., the reported water vapor integration time of 20 min was equivalent to a 33 min temporal resolution). Second, wavelength switching on timescales of several seconds can result in errors due to decorrelation between the online and offline signals from fluctuations in

Field deployable diode-laser-based DIAL for profiling water vapor

S. M. Spuler et al.

Title Page

Abstract

Introduction

Conclusions

References

Tables

Figures



Back

Close

Full Screen / Esc

Printer-friendly Version

Interactive Discussion



and offline throughput while minimizing angle tuning effects for the filter transmission at lower ranges that can affect the accuracy of the number density retrieval as discussed in Nehrir et al. (2009) and Wulfmeyer and Bösenberg (1998). Figure 2b shows the etalon transmission measurements and a fit to the data based on

$$T_{\text{etalon}} = \frac{(1 - R)^2}{1 + R^2 - 2R \cos \theta} \quad (1)$$

where, R is the etalon mirror reflectivity, and $\theta = 4\pi \frac{nL}{\lambda}$ is the round trip phase accumulation. The free spectral range (FSR) of the etalon is related to the optical cavity spacing by $\text{FSR} = \frac{c}{2nL}$ and was measured to be 0.0994 nm (43.3 GHz). The etalon was designed to allow transmission of the online and offline radiation in adjacent cavity modes. The finesse (F) of the etalon is related to the mirror reflectivity by $F = \frac{\pi\sqrt{R}}{1-R}$ yielding a finesse of $F = 43$. Figure 2c shows the combined passband for the far range receiver channel including both interference filters and the etalon.

The etalon is housed in a temperature controlled mount that integrates with the tube assembly housing of the receiver optics. A change in temperature of 22.4 °C is needed to tune the etalon through a full free spectral range. The operating temperature of the etalon is controlled via a thermoelectric cooler (TEC) using a commercial temperature controller with a temperature stability of 0.01 °C. The operating temperature of the etalon is adjusted to be resonant with the transmitted wavelengths. A plot of the resonant wavelength as a function of temperature is shown in the left panel of Fig. 3. The black circles represent measured values and the red line represents a linear fit showing a temperature tuning rate of $d\lambda/dT = 0.00441 \text{ nm}^\circ\text{C}^{-1}$. A plot of the cavity transmission as a function of finesse is shown on the right panel of Fig. 3. The locking stability of the injection seeding laser and the temperature stability of the etalon affects the etalon transmission. The effects of the locking stability on the cavity transmission can be modeled using the above equation with $\theta = \pi \frac{\Delta\lambda}{\text{FSR}_\lambda}$ where $\Delta\lambda$ is the detuning from the resonant peak in wavelength, and FSR_λ is the free spectral range in wavelength. The temperature stability of the etalon can be modeled using the measured

Field deployable diode-laser-based DIAL for profiling water vapor

S. M. Spuler et al.

Title Page

Abstract

Introduction

Conclusions

References

Tables

Figures



Back

Close

Full Screen / Esc

Printer-friendly Version

Interactive Discussion



temperature tuning rate, $d\lambda/dT$, through the above equation as well with $\theta = 2\pi \frac{d\lambda/dT \Delta T}{FSR_1}$ where $T = 0.01^\circ\text{C}$ is the temperature stability for the etalon.

Following the filters 90% of the received light is directed to a narrow field-of-view (FOV) fiber coupled detector module and 10% of the light to a free space receiver using a beam-splitting cube (as shown in Fig. 1). The light transmitted through the beam-splitting cube is incident on a 20 mm focal length lens focusing it onto a free-space avalanche photodiode (APD). The active area of the APD acts as the field stop resulting in a $451 \mu\text{rad}$ field-of-view. The light reflected from the beam-splitting cube passes through an interference filter with a 500 pm FWHM passband (passband is shown as the blue curve in Fig. 2a). The diameter of the beam is reduced approximately $4 \times$ with a beam reducing pair of optics (80 mm and 19 mm local length; respectively) to not exceed the numerical aperture (NA) of the fiber then focused with an 11 mm focal length lens into an multimode optical fiber with a $105 \mu\text{m}$ core diameter and a NA of 0.22. The optical fiber acts as the field stop producing a FOV of $115 \mu\text{rad}$. The optical fiber guides the received light to a fiber coupled APD.

For each detector module, full overlap occurs when the image of transmitted beam diameter is less than the diameter of the field stop. As shown in Fig. 4 the narrow field-of-view receiver (far range channel) has full overlap at ranges greater than 2.75 km, whereas the wide field-of-view receiver (or near range channel) achieves full overlap at approximately 700 m. The collected light has a r^{-2} dependence therefore the near range channel will have a larger signal at low ranges. However, it will also have substantially higher noise during daytime as it collects 16 times more background light compared to the far channel (solid angle $\propto \text{FOV}^2$). Thus only the lowest range gates of the wide field-of-view channel are useful during daytime. As discussed later, this receiver channel is most useful when operating the instrument at short temporal and spatial resolutions (e.g., 1 min and 75 m; respectively).

Field deployable diode-laser-based DIAL for profiling water vapor

S. M. Spuler et al.

Title Page

Abstract

Introduction

Conclusions

References

Tables

Figures



Back

Close

Full Screen / Esc

Printer-friendly Version

Interactive Discussion



2.4 Data acquisition and post processing

The output signal from the photon detection modules are connected to RF switches as shown in Fig. 1. The RF switch is used to separate the signals generated from the photon counting module between the online and offline transmitted laser pulses so as to eliminate the buffer crosstalk problem previously mentioned for the third generation system. A digital I/O counter tracks the number of pulses from the current pulse driver and sends a TTL state change to the pair of RF switches after a prescribed number of pulses are counted at each wavelength. In the standard configuration, the current pulse generator operates at 9 kHz, so there are 150 pulses at each wavelength with 60 Hz switching. The outputs of each RF switch are connected to two separate channels on the MCS. For near and far range all four channels of a 20 MHz MCS (Sigma Space Corporation) are used. 10 000 samples are accumulated with a bin duration of 500 ns and 220 bins for a maximum range of 16.5 km with 1.1 s acquisition time. The approximate 1 μ s pulse duration is over-sampled by the MCS, yielding 2 data points per 150 m, which corresponds to a sampled vertical range resolution of 75 m. The summing of these 75 m bins is performed during postprocessing where 2 bins are grouped together to yield a 150 m range resolution for the DIAL measurement.

Note that the large number of scattered photons from the outgoing pulse prohibits measuring the atmospheric return during the initial 1.1 μ s (i.e., while the current pulse is applied to the TSOA). Therefore, in the standard operational configuration, the lowest usable range gate is 225 m. However the current driver is easily reconfigurable so, for example, if it were programmed for a 500 ns duration pulse, the lowest usable gate could be reduced to 75 m range. The amplified laser pulse would be 300 ns in duration with roughly 1/3 of the energy per pulse.

Field deployable diode-laser-based DIAL for profiling water vapor

S. M. Spuler et al.

Title Page

Abstract

Introduction

Conclusions

References

Tables

Figures



Back

Close

Full Screen / Esc

Printer-friendly Version

Interactive Discussion



3 Model performance of a photon counting DIAL

In what follows, we consider a photon counting DIAL system. The precision of the water-vapor measurement can be estimated by the propagation of independent error in the DIAL equation given by

$$n_{\text{wv}}(r) = \frac{1}{2\Delta r(\sigma_{\text{on}}(r) - \sigma_{\text{off}}(r))} \ln \left[\frac{N_{\text{on}}(r)}{N_{\text{on}}(r + \Delta r)} \frac{N_{\text{off}}(r + \Delta r)}{N_{\text{off}}(r)} \right] \quad (2)$$

where n_{wv} is the number density of water vapor, Δr is the range bin size, σ is the absorption cross section at the online and offline wavelength (subscripts on, and off; respectively), and N is number of online and offline (subscripts on, and off; respectively) backscattered photons received.

The number of signal counts is given by

$$N_{\text{s}}(r, \lambda) = \frac{E\lambda A_{\text{r}}}{2h r^2} (\beta_{\text{a}}(r) + \beta_{\text{m}}(r)) \eta_{\text{r}} \eta_{\text{d}} O(r) \left[\exp \left(-2 \int_0^r (\alpha_{\text{a}} + \alpha_{\text{m}} + (\sigma(r, \lambda)) n_{\text{wv}}) dr \right) \right] \quad (3)$$

where E is the pulse energy of the laser, λ is the laser wavelength, h is the Planck constant, A_{r} is the area of the receiver telescope, β is the backscatter coefficient for aerosol and molecular (subscripts a and m; respectively), η is the efficiency of the receiver and detector (subscripts r and d; respectively), $O(r)$ is the overlap function, α is the extinction coefficient of the aerosol, molecular and water vapor (subscripts a, and m; respectively).

The number of background counts is given by

$$N_{\text{B}} = S_{\text{b}} \Omega_{\text{r}} \Delta_{\text{f}} A_{\text{r}} \eta_{\text{r}} \eta_{\text{d}} \frac{\lambda}{hc} \quad (4)$$

where S_{b} is the sky radiance, Ω_{r} is the receiver field-of-view solid angle, Δ_{f} is filter bandpass width, A_{r} is the area of the receiver telescope, η is the efficiency of the receiver and detector, and c is the speed of light.

Field deployable diode-laser-based DIAL for profiling water vapor

S. M. Spuler et al.

Title Page

Abstract

Introduction

Conclusions

References

Tables

Figures

◀

▶

◀

▶

Back

Close

Full Screen / Esc

Printer-friendly Version

Interactive Discussion



in Fig. 7, a two-way column OD of 0.6 and range bin of 600 m increases the maximum range of the instrument to about 7 km for a 5 % error.

A practical limit to the maximum range for the ground-based DIAL results from the small differential optical depth associated with the water vapor absorption in the free troposphere. The differential optical depth, $\Delta\tau$, needed to retrieve the water vapor number density (Wulfmeyer and Walther, 2001a) is $\Delta\tau = n\sigma_{\text{on}}\Delta R \approx 0.03\text{--}0.1$, where n is the water vapor number density, σ_{on} is the absorption cross section at the online wavelength, and R is the range bin size. For a maximum range bin size of 1 km, the maximum range at which the water vapor profile can be retrieved approaches 7 km.

Figure 8 shows the model results for a case with higher temporal and spatial resolution. For low level boundary layer studies, the instrument could be operated with a resolution of 75 m and 1 min as the near and far range channels could be combined to provide < 5 % error for the lowest 1.75 km. For a 75 m pulse length the duration of the TSOA current pulse would be reduced in half, from 1000 to 500 ns resulting in a pulse energy 2.6 μJ . It is possible that the pulse energy could be increased from the standpoint of eye-safety restrictions; however, a conservative TSOA pulse current of 10 A was assumed constant for this case. Any dataset can be processed to high temporal resolution a posteriori however reducing the pulse duration, and subsequently the power, to achieve higher spatial resolution needs to be considered more carefully.

4 Data examples and intercomparisons

The fourth generation diode-laser-based DIAL was constructed at the NCAR lab in Boulder, CO in four phases between October 2013 and June 2014, implementing (1) the shared telescope, (2) two channel receiver, (3) fast switching transmitter and receiver, and (4) the optimization of the background suppressing filters and etalon. During the 8 month period of development the instrument was run almost continuously with sonde comparisons done at each stage of the development. The completed instrument was moved to the Boulder Atmospheric Observatory (BAO) for operation

Field deployable diode-laser-based DIAL for profiling water vapor

S. M. Spuler et al.

Title Page

Abstract

Introduction

Conclusions

References

Tables

Figures



Back

Close

Full Screen / Esc

Printer-friendly Version

Interactive Discussion



**Field deployable
diode-laser-based
DIAL for profiling
water vapor**

S. M. Spuler et al.

Title Page

Abstract

Introduction

Conclusions

References

Tables

Figures



Back

Close

Full Screen / Esc

Printer-friendly Version

Interactive Discussion



4 km for the far-range channel. For this predominantly daytime set of comparisons, the near range channel provides a slightly lower error below 500 m range. The SD is $\approx 10\%$ about the mean at the surface and increases to $\approx 20\%$ at 1.5 km for the near-range channel and 4 km for the far-range channel. A small number of comparisons were greater than $3 \times$ SDs and were removed as outliers from the calculation of the mean. There are several potential reasons for discrepancies between the absolute humidity measured by the WV-DIAL and the radiosondes. The sondes inevitably drift with the wind as they rise and are generally not in close proximity to the lidar beam. Spatio-temporal matching was not employed at this phase in the analysis such as done in Vogelmann et al. (2011). Additionally, a strong wet-bias often occurs in the WV-DIAL at the cloud edges which is not filtered out in the current post-processing – as evidenced in the time vs. height profiles shown in Fig. 9. These spatially localized biases can dominate the statistics given the relatively small number of comparisons. More work will be done to remove these small regions of bias in the future. And finally, there may be systematic instrument bias or errors within the HITRAN 2008 molecular spectroscopic database parameters used to calculate the differential absorption cross section of the water molecule. To improve performance, detailed studies of the molecular spectroscopic parameters have been performed for other DIAL systems – such as those presented by Grossmann and Browell (1989), Lisak et al. (2009) and Ponsardin and Browell (1997) – and may be required to improve the accuracy of this system. With these caveats, it seems reasonable to claim that the measurements of water vapor provided by the WV-DIAL agree well (with less than 10 % mean error) with the radiosonde measurements of water vapor over a wide range of atmospheric conditions.

The instrument was operated unattended for 50 continuous days during the FRAPPE field campaign from a mobile laboratory container with approximately $\pm 5^\circ\text{C}$ temperature stability. The device was aligned once (at setup only) and there was no detectable degradation in performance during the project or evidence of temperature cycling in the data. The instrument operated reliably – providing $> 95\%$ data coverage. A subset – a two week period from 1–14 July 2014 – of near continuous data is shown as Fig. 11.

**Field deployable
diode-laser-based
DIAL for profiling
water vapor**

S. M. Spuler et al.

Title Page

Abstract

Introduction

Conclusions

References

Tables

Figures



Back

Close

Full Screen / Esc

Printer-friendly Version

Interactive Discussion



- Ponsardin, P. L. and Browell, E. V.: Measurements of H₂¹⁶O linestrengths and air-induced broadenings and shifts in the 815 nm spectral region, *J. Mol. Spec.*, 185, 58–70, 1997. 11283
- Reagan, J. A., Cooley, T. W., and Shaw, J. A.: Prospects for an economical, eye-safe water vapor LIDAR, in: *International Geoscience and Remote Sensing Symposium, Better Understanding of Earth Environment*, IEEE, Kogakuin University, Tokyo, Japan, 872–874, doi:10.1109/IGARSS.1993.322198, 1993. 11268
- Repasky, K., Moen, D., Spuler, S., Nehrir, A., and Carlsten, J.: Progress towards an autonomous field deployable diode-laser-based Differential Absorption Lidar (DIAL) for profiling water vapor in the lower troposphere, *Remote Sensing*, 5, 6241–6259, doi:10.3390/rs5126241, 2013. 11269, 11270, 11281
- Rothman, L., Gordon, I., Barbe, A., Benner, D., Bernath, P., Birk, M., Boudon, V., Brown, L., Campargue, A., Champion, J.-P., Chance, K., Coudert, L., Dana, V., Devi, V., Fally, S., Flaud, J.-M., Gamache, R., Goldman, A., Jacquemart, D., Kleiner, I., Lacome, N., Lafferty, W., Mandin, J.-Y., Massie, S., Mikhailenko, S., Miller, C., Moazzen-Ahmadi, N., Naumenko, O., Nikitin, A. V., Orphal, J., Perevalov, V., Perrin, A., Predoi-Cross, A., Rinsland, C., Rotger, M., Šimečková, M., Smith, M., Sung, K., Tashkun, S., Tennyson, J., Toth, R., Vandaele, A. C., and Vander Auwera, J.: The HITRAN 2008 molecular spectroscopic database, *J. Quant. Spectrosc. Ra.*, 110, 533–572, doi:10.1016/j.jqsrt.2009.02.013, 2009. 11268, 11281
- Turner, D. D. and Löhnert, U.: Information content and uncertainties in thermodynamic profiles and liquid cloud properties retrieved from the ground-based Atmospheric Emitted Radiance Interferometer (AERI), *J. Appl. Meteorol. Clim.*, 53, 752–71, 2014. 11267
- Turner, D. D., Ferrare, R. A., Brasseur, L. A. H., Feltz, W. F., and Tooman, T. P.: Automated retrievals of water vapor and aerosol profiles from an operational Raman lidar, *J. Atmos. Ocean. Tech.*, 19, 37–50, 2002. 11267
- Vaughan, J. M., Brown, D. W., Nash, C., Alejandro, S. B., and Koenig, G. G.: Atlantic atmospheric aerosol studies 2. Compendium of airborne backscatter measurements at 10.6 μm, *J. Geophys. Res.*, 100, 1043–1065, 1995. 11291
- Vogelmann, H. and Trickl, T.: Wide-range sounding of free-tropospheric water vapor with a differential-absorption lidar (DIAL) at a high-altitude station, *Appl. Optics*, 47, 2116, doi:10.1364/AO.47.002116 2008. 11268
- Vogelmann, H., Sussmann, R., Trickl, T., and Borsdorff, T.: Intercomparison of atmospheric water vapor soundings from the differential absorption lidar (DIAL) and the solar FTIR system on Mt. Zugspitze, *Atmos. Meas. Tech.*, 4, 835–841, doi:10.5194/amt-4-835-2011, 2011. 11283

Field deployable diode-laser-based DIAL for profiling water vapor

S. M. Spuler et al.

Table 2. Model atmosphere parameters used to calculate the performance.

Daytime sky radiance	$1.15 \times 10^{-3} \text{ W cm}^{-2} \mu\text{m}^{-1} \text{ sr}^{-1}$
Aerosol lidar ratio	50 sr
Molecular lidar ratio	$8/3\pi$ sr
Molecular backscatter coefficient	Fig. 5 (left panel)
Aerosol backscatter coefficient	Fig. 5 (left panel) data from Vaughan et al. (1995)
Water vapor concentration profile	Fig. 5 (right panel) data from Wulfmeyer and Walther (2001b)

Title Page

Abstract

Introduction

Conclusions

References

Tables

Figures



Back

Close

Full Screen / Esc

Printer-friendly Version

Interactive Discussion



AMTD

7, 11265–11302, 2014

Field deployable diode-laser-based DIAL for profiling water vapor

S. M. Spuler et al.

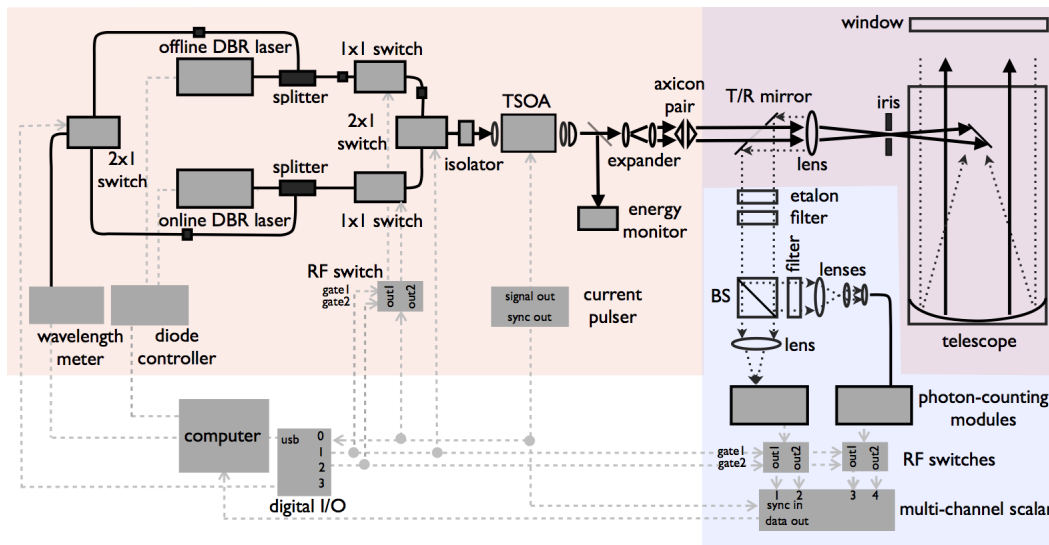


Figure 1. Schematic of the WV-DIAL system. BS = beam-splitter; T/R = transmit receive; I/O = input output.

Title Page

Abstract Introduction

Conclusions References

Tables Figures

◀ ▶

◀ ▶

Back Close

Full Screen / Esc

Printer-friendly Version

Interactive Discussion



Field deployable diode-laser-based DIAL for profiling water vapor

S. M. Spuler et al.

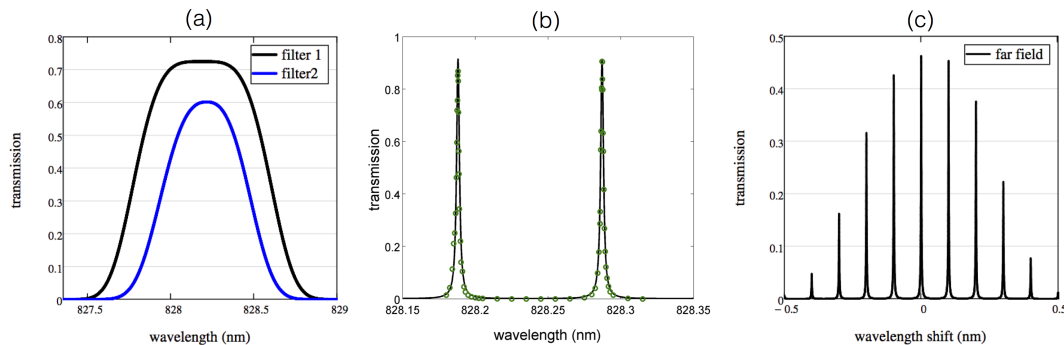


Figure 2. The multi-stage optical filtering enabling measurement of water vapor during daytime bright-cloud conditions. **(a)** shows the interference filter transmission as a function of wavelength. The solid black (blue) line is a fit to the measured filter transmission for the FWHM bandpass of 750 pm (500 pm). A double cavity design was used for both filters to provide a more flat passband. The wider filter is common to both the near and far range channels while the narrower filter is used only in the far range channel. **(b)** shows the etalon transmission as a function of wavelength. The green circles represent measured values while the solid black line represents a fit. **(c)** shows the combined passband for the far range channel including both interference filters and the etalon.

[Title Page](#)[Abstract](#)[Introduction](#)[Conclusions](#)[References](#)[Tables](#)[Figures](#)[◀](#)[▶](#)[◀](#)[▶](#)[Back](#)[Close](#)[Full Screen / Esc](#)[Printer-friendly Version](#)[Interactive Discussion](#)

Field deployable diode-laser-based DIAL for profiling water vapor

S. M. Spuler et al.

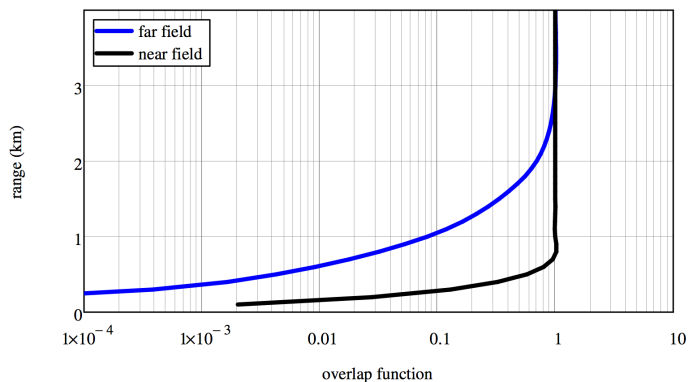


Figure 4. Overlap function for the far and near range receiver channels calculated from an optical model of the instrument.

[Title Page](#)[Abstract](#)[Introduction](#)[Conclusions](#)[References](#)[Tables](#)[Figures](#)[◀](#)[▶](#)[◀](#)[▶](#)[Back](#)[Close](#)[Full Screen / Esc](#)[Printer-friendly Version](#)[Interactive Discussion](#)

Field deployable diode-laser-based DIAL for profiling water vapor

S. M. Spuler et al.

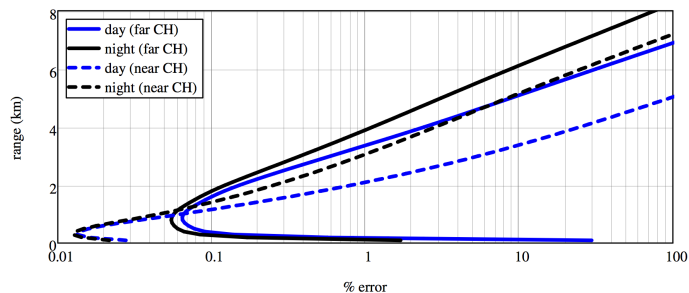


Figure 6. Performance estimate for day and night with 150 m range resolution for the near and far range channels for an online column OD of 1.5. For a 5% error, the instrument has a maximum daytime range of ≈ 5 km.

Title Page

Abstract

Introduction

Conclusions

References

Tables

Figures

◀

▶

◀

▶

Back

Close

Full Screen / Esc

Printer-friendly Version

Interactive Discussion



Field deployable diode-laser-based DIAL for profiling water vapor

S. M. Spuler et al.

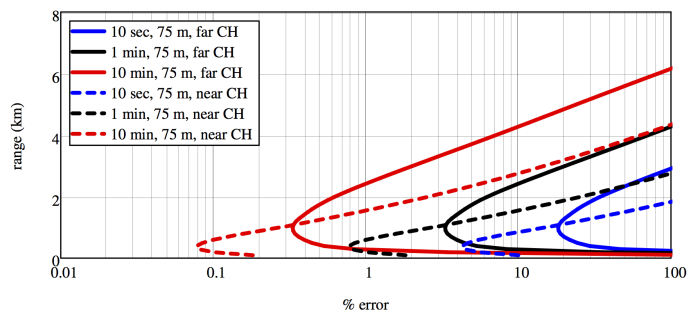


Figure 8. Daytime performance estimate in % error for temporal resolutions of 10 s, 1, and 10 min with a spatial resolution of 75 m for an online column OD of 1.5. The pulse energy is half – $2.6 \mu\text{J}$ – for this case because of the shorter pulse duration. These model results indicate that 1 min, 75 m resolution may be useful for boundary layer studies.

Title Page

Abstract

Introduction

Conclusions

References

Tables

Figures



Back

Close

Full Screen / Esc

Printer-friendly Version

Interactive Discussion



Field deployable diode-laser-based DIAL for profiling water vapor

S. M. Spuler et al.

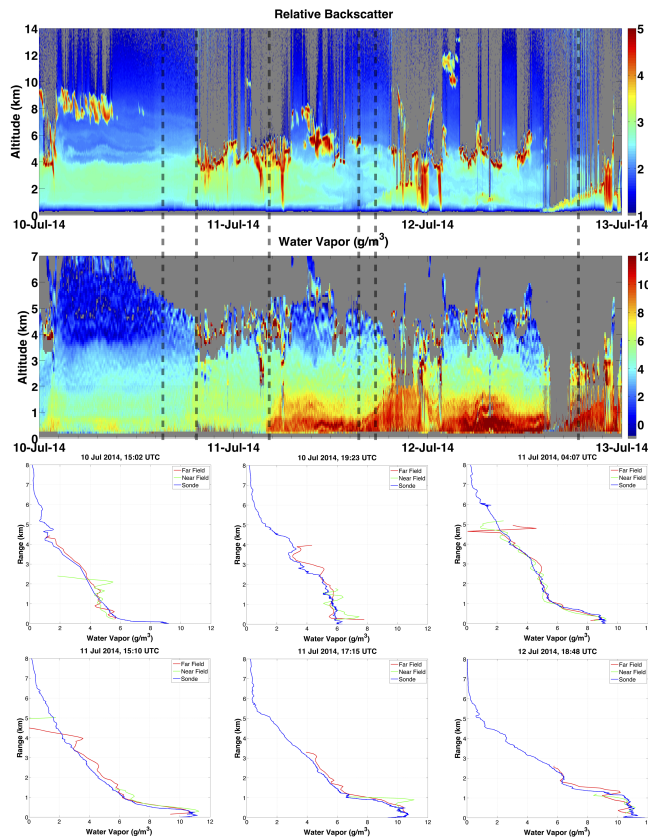


Figure 9. Top panels: 1 min, 150 m resolution relative backscatter from 0–14 km range; bottom panels: 1 min, 150 m resolution water vapor in g m^{-3} from 0–2 km range, and 10 min, 150 m resolution from 2–7 km. Far range channel. The dashed black lines indicate times when the sondes were launched. The individual water vapor concentration profiles are shown on the bottom for the sonde (blue), far range (red) and near range channel (green) in g m^{-3} .

[Title Page](#)
[Abstract](#)
[Introduction](#)
[Conclusions](#)
[References](#)
[Tables](#)
[Figures](#)
[Back](#)
[Close](#)
[Full Screen / Esc](#)
[Printer-friendly Version](#)
[Interactive Discussion](#)

Field deployable diode-laser-based DIAL for profiling water vapor

S. M. Spuler et al.

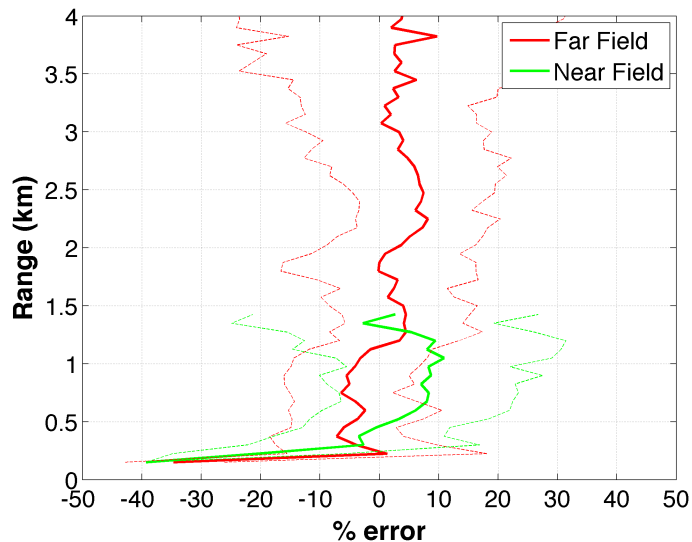


Figure 10. Sonde to DIAL measured water vapor in percent error. The mean (solid line) and SD (dashed line) percent errors are shown for all 45 sondes launched from 10 July through 19 August. The spatial resolution of the DIAL profiles are 150 m below 2 km and 600 m above 2 km. The DIAL profiles were processed with at 1 min temporal resolution and averaged for 25 min starting at the sonde launch time.

[Title Page](#)[Abstract](#)[Introduction](#)[Conclusions](#)[References](#)[Tables](#)[Figures](#)[◀](#)[▶](#)[◀](#)[▶](#)[Back](#)[Close](#)[Full Screen / Esc](#)[Printer-friendly Version](#)[Interactive Discussion](#)

Field deployable diode-laser-based DIAL for profiling water vapor

S. M. Spuler et al.

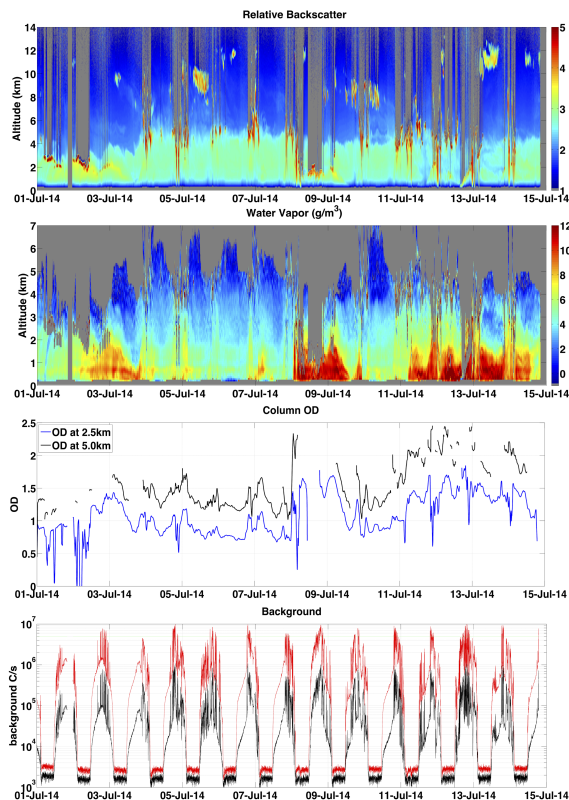


Figure 11. Two weeks of near continuous data collected 1–14 July 2014. Top panel: 1 min, 150 m resolution relative backscatter from 0 to 14 km range for the far range channel; second panel from top: 10 min, 150 m resolution water vapor in g m^{-3} from 0 to 7 km range for the far range channel, second panel from bottom: measured two-way optical depth at 2.5 km (blue) and 5.0 km (black) range for the far range channel; and bottom panel: background in counts per second (C s^{-1}) for the near (red) and far (black) range channels.

[Title Page](#)[Abstract](#)[Introduction](#)[Conclusions](#)[References](#)[Tables](#)[Figures](#)[◀](#)[▶](#)[◀](#)[▶](#)[Back](#)[Close](#)[Full Screen / Esc](#)[Printer-friendly Version](#)[Interactive Discussion](#)